Targeting RAS Mutant Colorectal Cancer with Dual Inhibition of MEK and CDK4/6

Alexey V. Sorokin[1], Preeti Kanikarla Marie[1], Lea Bitner[1], Muddassir Syed[1], Melanie Woods[1], Ganiraju Manyam[2], Lawrence N. Kwong[3], Benny Johnson[1], Van K. Morris[1], Philip Jones[4], David G. Menter[1], Michael S. Lee[1], and Scott Kopetz[1]

ABSTRACT

KRAS and NRAS mutations occur in 45% of colorectal cancers, with combined MAPK pathway and CDK4/6 inhibition identified as a potential therapeutic strategy. In the current study, this combinatorial treatment approach was evaluated in a co-clinical trial in patient-derived xenografts (PDX), and safety was established in a clinical trial of binimetinib and palbociclib in patients with metastatic colorectal cancer with RAS mutations. Across 18 PDX models undergoing dual inhibition of MEK and CDK4/6, 60% of tumors regressed, meeting the co-clinical trial primary endpoint. Prolonged duration of response occurred predominantly in TP53 wild-type models. Clinical evaluation of binimetinib and palbociclib in a safety lead-in confirmed safety and provided preliminary evidence of activity. Prolonged treatment in PDX models resulted in feedback activation of receptor tyrosine kinases and acquired resistance, which was reversed with a SHP2 inhibitor. These results highlight the clinical potential of this combination in colorectal cancer, along with the utility of PDX-based co-clinical trial platforms for drug development.

Significance: This co-clinical trial of combined MEK-CDK4/6 inhibition in RAS mutant colorectal cancer demonstrates therapeutic efficacy in patient-derived xenografts and safety in patients, identifies biomarkers of response, and uncovers targetable mechanisms of resistance.

Introduction

Colorectal cancer is currently the second leading cause of cancer-related death in the United States, which continues to increase in the young and underserved (1). KRAS mutations comprise 86% of all RAS pathway aberrations that are present in roughly 20%, of all human malignancies and have centered of late on G12C variants (2). The incidence of KRAS and NRAS mutations (RAS^{mut}) in colorectal cancer is especially high (>40%) as well as more common in right-sided tumors along with frequent occurrences in consensus molecular subtype 3 (CMS3) tumors (3, 4). Cetuximab and panitumumab, EGFR inhibitors approved for clinical use against mCRC, provide no benefit to patients with $KRAS^{mut}$ and $NRAS^{mut}$ tumors (5, 6). As a result, RAS^{mut} tumors remain a critical unmet need for drug development.

Oncogenic RAS can induce cell proliferation, increase motility, reduce contact inhibition, alter metabolism, and degrade genome integrity (7, 8), which frequently culminates in oncogene addiction. KRAS and NRAS have long been considered "undruggable" due to strong affinity for GTP and lack of deep, targetable binding sites (9). In recent years however, small molecules were engineered to covalently couple to $KRAS^{G12C}$ mutations in the P-loop domain that disrupt the switch II protein domain, thereby trapping the overall molecule in the inactive GDP-bound state (10). Inhibitors of $KRAS^{G12C}$ have shown promise, but this mutation is only present in 2% to 4% of colorectal cancer. The success and prospective advantages of direct $KRAS^{G12C}$ specific inhibitors have reinvigorated this field. This revival has emphasized a focus on the molecular changes and key interactions associated with specific RAS mutations, and a need to understand adaptive responses to treatment (11).

Alternative and compensatory strategies for treating RAS^{mut} tumors involve complex RAS-mediated feedback loop and compensatory signal transduction mechanisms. While inhibition of MEK has not been effective *in vivo*, rational combinations have been proposed based on synergistic pathways. One such combination involves cyclin-dependent kinase 4/6 (CDK4/6) inhibitors, which block the transition from the G_1 to S-phase of the cell cycle by interfering with RB (12). It was previously shown that the combination of MEK and CDK4/6 inhibition might inhibit the growth benefit of $KRAS^{mut}$ induction in a genetically engineered melanoma mouse model based on synthetic lethal extinction (13). Within this same vein of thought, we and others previously reported that combining a MEK inhibitor (trametinib) with CDK4/6 inhibitor (palbociclib) resulted significant synergy in inhibiting $KRAS^{mut}$ colorectal cancer growth (14, 15). However, robust preclinical work to understand the breadth of potential benefit across a population of colorectal cancer and potential predictors of response are needed. To address this gap, we have tested the breadth and duration of activity of the combination in a wide spectrum of patient-derived xenografts (PDX) models and evaluated novel mechanisms of resistance. These models benefit from maintaining the intratumoral heterogeneity and molecular features found in human tumors, and therefore provide a more translatable assessment of clinical response or mechanisms of resistance (16–19). While trametinib and binimetinib used in this study target the same molecule (MEK1/2), they differ

[1]Department of Gastrointestinal Medical Oncology, The University of Texas MD Anderson Cancer Center, Houston, Texas. [2]Department of Bioinformatics and Computational Biology, The University of Texas MD Anderson Cancer Center, Houston, Texas. [3]Department of Translational Molecular Pathology, The University of Texas MD Anderson Cancer Center, Houston, Texas. [4]Institute for Applied Cancer Science, The University of Texas MD Anderson Cancer Center, Houston, Texas.

A.V. Sorokin and P. Kanikarla Marie contributed equally as co-first authors.

Corresponding Author: Scott Kopetz, Department of Gastrointestinal Medical Oncology, The University of Texas MD Anderson Cancer Center, 1515 Holcombe Blvd., Unit 426, Houston, TX 77030. Phone: 713-792-2828; E-mail: skopetz@mdanderson.org

Cancer Res 2022;82:3335–44

doi: 10.1158/0008-5472.CAN-22-0198

This open access article is distributed under the Creative Commons Attribution-NonCommercial-NoDerivatives 4.0 International (CC BY-NC-ND 4.0) license.

©2022 The Authors; Published by the American Association for Cancer Research

in their pharmacokinetics and half-lives. Both have been evaluated in combinations in colorectal cancer, although they are not currently FDA approved for any colorectal cancer indications. The current study focuses on using a comprehensive series of RAS^{mut} colorectal cancer PDX models to: (i) identify biomarkers of response/resistance to the MEK/CDK4/6 inhibitor combination; (ii) reveal the safety of the combination in patients; and (iii) explore key mechanisms of resistance and novel actionable clinical targets.

Materials and Methods

Materials

NOD/SCID and 69 athymic nude mice were purchased from The Jackson Laboratory and from Envigo Rms, Inc., respectively. All drugs (except LY3214996, and Navire 13909) were received via CTEP agreement (U54 NCI). LY3214996 was purchased from MedChem Express. Navire 13909 (SHP2 inhibitor) was kindly provided by Navire Pharma under an MTA. All drugs (except palbociclib) were dissolved in dimethyl sulfoxide (DMSO) and stored at −20°C. For *in vivo* experiments, all drugs were prepared fresh daily from DMSO stocks or powder (for palbociclib). List of antibodies and other reagents used in this study are provided in Supplementary Table S1.

In vivo studies and PDXs

All *in vivo* experiments and procedures were approved by Institutional Animal Care and Use Committee. All *in vivo* experiments utilizing PDXs were performed according to NIH NCI recommendations summarized in SOP50102: PDX Implantation, Expansion and Cryopreservation (Subcutaneous). Primary human–tumor xenograft models were established as described previously (20). Tumor specimens were obtained from patients with mCRC under a research laboratory protocol approved by UT MD Anderson Cancer Center Institutional Review Board (IRB), and all patients provided written informed consent for specimens to be used for research purposes including implantation in xenografts. Xenografts were established in 6- to 8-week-old female NSG mice. Once established, PDXs were expanded in 69 athymic nude mice for experiments. After tumors were established with median tumor volume exceeding 200 to 250 mm^3, treatment of 10 mice/arm was commenced via oral gavage with either vehicle control (0.5% Tween 80/0.5% CMC in water), or drug/combinations as indicated in figure legends. Tumor size and mouse weight were measured twice a week. Study endpoints were determined by the duration of treatments. Any unexpected health conditions in mice, excessive tumor burden (more than 2 cm in diameter), or body weight loss exceeding greater than 20% were taken into consideration for early humane endpoints in this study. This study utilized nude mice in all experiments as we and others have observed that rates of engrafment for GI tumors is relatively high in these mice (21). Nude mice also allow for easy observation of subcutaneous tumors. In addition, we have previously observed concordance between responses in preclinical PDX studies utilizing nude mice and clinical trial observations (22). Tumors from three mice per arm were excised (2–4 hours posttreatment), segmented, and immediately flash frozen in liquid nitrogen (for protein, RNA, and DNA analysis) or 10% buffered formalin solution (for IHC staining). PDX model details are provided in Supplementary Table S1.

Clinical trial

A phase II clinical trial of the MEK inhibitor binimetinib and the CDK4/6 inhibitor palbociclib was initiated in patients with $KRAS^{mut}$ and $NRAS^{mut}$ mCRC who were previously treated with and refractory to standard 5-fluorouracil, irinotecan, oxaliplatin, and antiangiogenic therapies (NCT03981614, ClinicalTrials.gov). We prespecified a 6-subject safety run-in cohort to confirm the safety and tolerability of the recommended phase II dose of binimetinib 30 mg orally twice per day continuously and palbociclib 100 mg orally once daily on days 1 to 21 out of a 28-day cycle, as determined in a preceding dose escalation study in lung cancer (NCT03170206). We specified that if only 0 to 1 of the 6 subjects experienced a predefined excessive toxicity event, then we would deem the combination tolerable and proceed with further enrollment on our phase II study, while if 2 or more subjects experienced an excessive toxicity event, then we would enroll an additional 6 subjects for tolerability with dose de-escalation. Six patients were to be treated at each dose level and observed for a minimum of 28 days from cycle 1 day 1 to cycle 1 day 28. All patients who received the assigned treatment were considered evaluable for toxicities to make a dose escalation decision. We prespecified excessive toxicity events reflecting the known and expected toxicities of binimetinib and palbociclib. Events meeting criteria for excessive toxicity during the safety run-in will were defined as an adverse event or abnormal laboratory value assessed as at least possibly related to binimetinib and/or palbociclib that occurs during the first 28 days of treatment and fulfills any of the criteria as in Supplementary Table S2. Toxicity was evaluated according to the NCI CTCAE v4.03. Whenever a patient experienced toxicity that fulfilled the criteria for an excessive toxicity event, treatment with the study drug was interrupted and the toxicity was followed up.

The trial was designed per CONSORT guidelines and conducted with IRB approval, with written informed consent obtained from all subjects, and in accordance with U.S. Common Rule. Binimetinib was administered at 30 mg twice a day, daily days 1 to 28, and palbociclib at 100 mg daily on days 1 to 21 of 28-day cycle.

Other methods

Other methods are included in Supplementary Materials and Methods.

Data availability

The data generated in this study are available within the article and its Supplementary Data files. Raw reverse-phase protein arrays (RPPA) data for this study were generated at UT MD Anderson Cancer Center's RPPA Core. Derived data supporting the findings of this study are available from the corresponding author upon request.

Results

Combined inhibition of MEK and CDK4/6 in colorectal cancer PDX models

Previous studies showed that combining MEK and CDK4/6 inhibitors had synergistic antitumor activity predominantly in $KRAS^{mut}$ colorectal cancer cell lines, but robust assessment in PDX models in a formal preclinical study has not been conducted (14). To determine activated pathways that could inform targeting strategies, we performed RPPA analysis on our RAS^{mut} and wild-type RAS (RAS^{WT}) mCRC PDXs. We confirmed significant RAS/MAPK cascade activation (pMEK1/2 T202 $P = 0.002$) in PDX models with KRAS mutated in codons 12/13 compared with PDX models with RAS^{WT} gene or other RAS^{mut} (**Fig. 1A**). On the basis of this finding, we evaluated typical RAS models that include a mixture of exon 2 $KRAS^{G12/13}$ ($n = 6$) P-loop domain mutated PDX models, extended RAS models that include $NRAS^{Q61}$ switch II domain mutated tumors ($n = 2$) along with

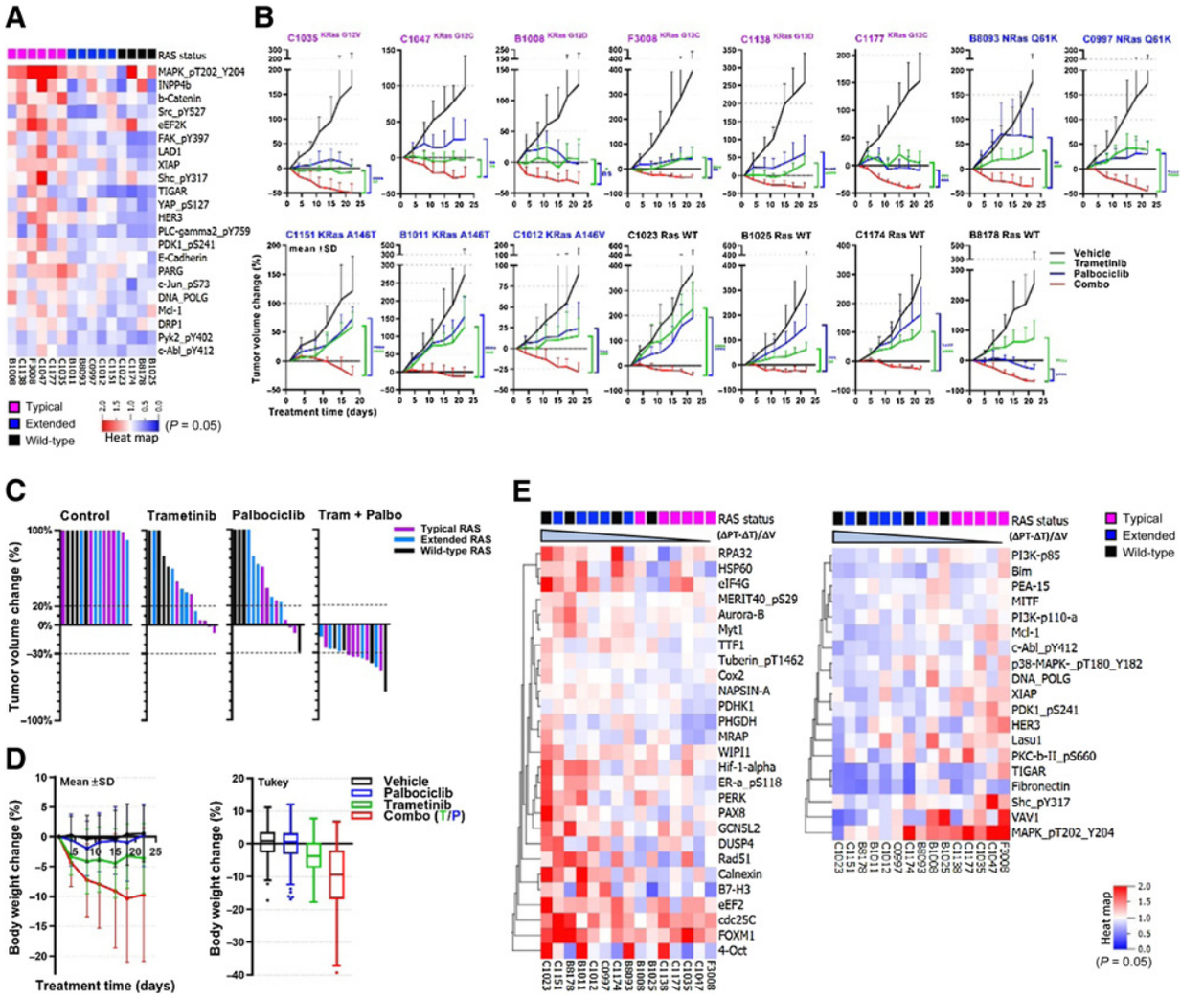

Figure 1.

Evaluation of trametinib/palbociclib combination in mCRC PDX models with different mutational RAS status. **A,** Relative baseline protein expression level in mCRC PDX models. Six PDX models harboring codon 12 or 13 ("typical" RAS), 5 with codons 61 or 149 mutations ("extended" RAS), and 4 wild-type RAS PDX models were analyzed by RPPA ("baseline," untreated tumors; $P < 0.05$, two-group comparison: codon 12/13 vs. others). **B,** Effect of treatments on tumor volume change (mean ± SD; $n = 6$–9 tumors per arm). Trametinib (0.25 mpk, daily; green), palbociclib (75 mpk, daily; blue), and their combination (red) were evaluated in 15 mCRC PDX models. ns, nonsignificant, $P > 0.05$; *, $P \le 0.05$; **, $P \le 0.01$; ***, $P \le 0.001$; ****, $P \le 0.0001$. **C,** Waterfall representation of 15 PDX models' responses, per PDX model results. **D,** Effect of treatments on mice body weight. Right, Tukey plot, after 21 days of treatment. Summarized data for 15 PDX models. **E,** Relative baseline protein expression level in mCRC PDX models ranked by magnitude in response to the combination relative to trametinib response ($P < 0.05$, linear regression analysis).

$KRAS^{A146T}$ nucleotide exchange promoting domain mutated tumors ($n = 3$; refs. 23, 24), and wild-type RAS tumors ($n = 4$).

The PDX co-clinical trial of MEK (trametinib) and CDK4/6 (palbociclib) inhibition met its prespecified primary endpoint of tumor regression of ≥30% in more than 30% of the models. As shown in **Fig. 1B** and **C**, the combination of MEK and CDK4/6 inhibition produced ≥30% regression in 9 of 15 models (60%) with significantly greater tumor growth inhibition when compared with single agent–treated PDXs. Models with typical RAS mutations had greater growth inhibition with single-agent MEK inhibition than extended RAS mutations or RAS^{WT} models. In contrast, with the combination, there was efficacy seen across all RAS subgroups. The combination caused modest weight loss in mice that was experimentally manageable (**Fig. 1D**).

Markers of synergy in response to MEK and CDK4/6 combination

Characterization of synergism responses was achieved by ranking PDX models by the magnitude of their *in vivo* volume change to the combination relative to trametinib response [Supplementary Table S3, ranked by (ΔPT-ΔT)/ΔV values)]. When compared with typical RAS^{mut} models, codon extended RAS^{mut} ($P < 0.001$) or RAS^{WT} ($P = 0.01$) models had greater degree of benefit with the addition of palbociclib.

Next, we linked our RAS model subtype distribution by response-based rank order to baseline protein levels (**Fig. 1E**). In the models that benefitted the most from palbociclib combination, there was a significant enrichment in cell-cycle regulators (e.g., Aurora B, CDC25C, Myt1, etc.) and transcriptional factors that modulate cell proliferation,

self-renewal, and tumorigenesis (e.g., OCT4, FOXM1). Correlation matrix shows clustering of these protein levels as well (Supplementary Fig. S1). These models also had a significantly less active RAS/MAPK axis [phospho-Erk1/2 (T202/Y204), phospho-p38/MAPK (T180/Y182), VAV1, PEA15; **Fig. 1E**, $P < 0.05$, FDR < 0.05].

Drug target engagement evaluation

Target engagement was then examined using Western blotting and IHC staining in the F3008 model, which demonstrated moderate activity with single agents, and B1011, which did not have single-agent activity. As expected, phospho-MAPK1/2 and phospho-RB1 levels were strongly decreased after trametinib or palbociclib treatment, respectively, in the single agent–responding F3008 model but not in the nonresponding B1011 model. In contrast, phosphor-MAPK1/2 and phosphor-RB1 were strongly suppressed in both models when treated with the combination, consistent with the regression seen in both PDXs (Supplementary Fig. S2A and S2B). We also performed RPPA on all tumor samples after 5 days and 21 days of treatments. Summarized data on signaling molecule changes are presented in Supplementary Fig. S3 and Supplementary Table S4. The response to palbociclib occurred within 5 days and was sustained at the same level for 21 days (Supplementary Table S4A and S4B). Meanwhile adequate target inhibition with trametinib was seen at the latter time point. Interestingly, we observed some upregulation in phospho-Akt and phospho-S6 levels after day 21 of treatment with the combination (comparing with day 5), indicating that Akt signaling pathway may mediate adaptation after prolonged treatment (Supplementary Fig. S3; Supplementary Table S4B).

Optimization of MEK and CDK4/6 combination therapy

With combination regimens, the selection of which drug to dose-reduce in the clinic in the setting of adverse events is typically made on the basis of toxicity profiles without consideration of impact on the efficacy tradeoff. Acknowledging the potential for toxicities of the combination in the clinic, we sought to understand optimal dose reductions that could maintain efficacy while reducing certain toxicities.

A dose/response matrix analyses was established based on reductions in dose for both palbociclib and trametinib (**Fig. 2A** and **B**). These results demonstrate that reducing palbociclib dose provides reduced toxicity (as reflected in body weight changes, **Fig. 2B**) with more modest impacts on treatment efficacy (**Fig. 2A**). CBC profile of mice also revealed that toxicity in the combination was mediated mainly by palbociclib (Supplementary Table S5). To evaluate alternate strategies of palbociclib dose reduction, we treated three PDX models (one of each RAS subtype) with various dosing regimens of palbociclib to optimize combinatorial efficacy based on tumor volume changes and limit toxicity based on weight changes. **Figure 2C** panels show tumor volume change in these three PDX models with various palbociclib dosing regimens. The bottom panels show how efficacy of the adjusted dose compares with that of the full dose (estimated at 100%, see also Supplementary Table S6). Better tolerance to treatment was also observed with improved body weight changes within the acceptable range (**Fig. 2D**). **Figure 2E** suggests that by modest drop in palbociclib dose, we can maintain body weight with limited reduction in efficacy, and that this toxicity–efficacy trade off was more favorable than a dose reduction in trametinib. Here, we focused on weight loss and cytopenia, and evaluated not just toxicity, but toxicity and efficacy tradeoffs. In this setting, the data suggested that palbociclib dose reductions would improve toxicity with less impact on efficacy than reductions in MEK, which also resulted in improved toxicity but also more negative impact on efficacy. Initial palbociclib dose reduction was incorporated as the preferred dose adjustment strategy in the randomized phase II clinical trial.

Combined MEK and CDK4/6 inhibition is tolerable and translates to response in colorectal cancer

The combination of the MEK inhibitor binimetinib and the CDK4/6 inhibitor has been demonstrated to be well tolerated in a 3 + 3 dose escalation phase I trial (NCT03170206), with a recommended phase II dose of binimetinib 30 mg orally twice per day continuously and palbociclib 100 mg orally once daily on days 1 to 21 out of a 28-day cycle (personal communication). We studied this regimen in a prospectively defined 6-subject safety run-in of a randomized phase II clinical trial of binimetinib and palbociclib in *KRAS*- or *NRAS*-mutant metastatic colorectal cancer patients (NCT03981614). During the predefined toxicity-monitoring period of the first 28 days of combination treatment, treatment was well tolerated, with only one subject experiencing a predefined excessive toxicity (grade 3 oral mucositis; Supplementary Table S2). These doses are being used for further enrollment on the randomized portion of the trial, with no subsequent changes required to the binimetinib and palbociclib regimen.

Highlighting the potential clinical benefit of the combination, in the safety lead-in, a patient with a $KRAS^{G12D}$ mutated mCRC previously treated with multiple prior therapies, including 5-fluorouracil, oxaliplatin, irinotecan, and bevacizumab had a confirmed PR, with 46% reduction in two target lesions in the liver at first restaging and radiographic resolution of low-volume nontarget lung nodules (**Fig. 3A**), accompanied by a reduction in circulating CEA levels (**Fig. 3B**).

Markers of MEK and CDK4/6 inhibitors treatment durability

When using progression-free survival (PFS) as an important and primary endpoint to assess durability of a drug response, eight PDX models (4 of each RAS^{mut} subtype) were treated beyond 21 days using the trametinib/palbociclib 5 days on, 2 days off dose regimen. **Figure 4A** shows the tumor volume changes with prolonged treatment, each line representing individual tumor. Impact of continuous treatment was measured as PFS, calculated as the time in days for doubling of the tumor volume under constant dosing for individual PDX models (**Fig. 4B**). There was no difference in PFS between typical RAS^{mut} and extended RAS^{mut} models treated with the combination (**Fig. 4C**, median survival: 47 vs. 55 days, ns). The consensus molecular subtypes (CMS) have previously been shown to be predictive for EGFR inhibition benefit and were explored as potential predictive biomarker. When compared to CMS subtype analyses, CMS2 subtype tumors benefited longer from the treatment compared with CMS3 (**Fig. 4D**, median survival: 36 vs. 66 days, $P = 0.0001$).

To identify potential protein biomarkers that might associate with combination durability we separated PDX models into two groups by their ratio of median PFS (untreated vs. on treatment, **Fig. 4E**) and performed analysis of baseline protein levels and mutations in these two groups (**Fig. 4F**; Supplementary Fig. S4). Models with short durability had higher phospho RB levels and Wee1 overexpression. Stratification by TP53 status demonstrated that tumors with TP53 mutations had shorter PFS (**Fig. 4G**, median survival: 40.5 vs. 83 days, $P = 0.05$, Supplementary Table S7). Other potential biomarkers or markers of interest include OCT4 protein, a common marker for undifferentiated or stem-like cells, and claudin-7, which were overexpressed in tumors with short duration of disease control (**Fig. 4F**).

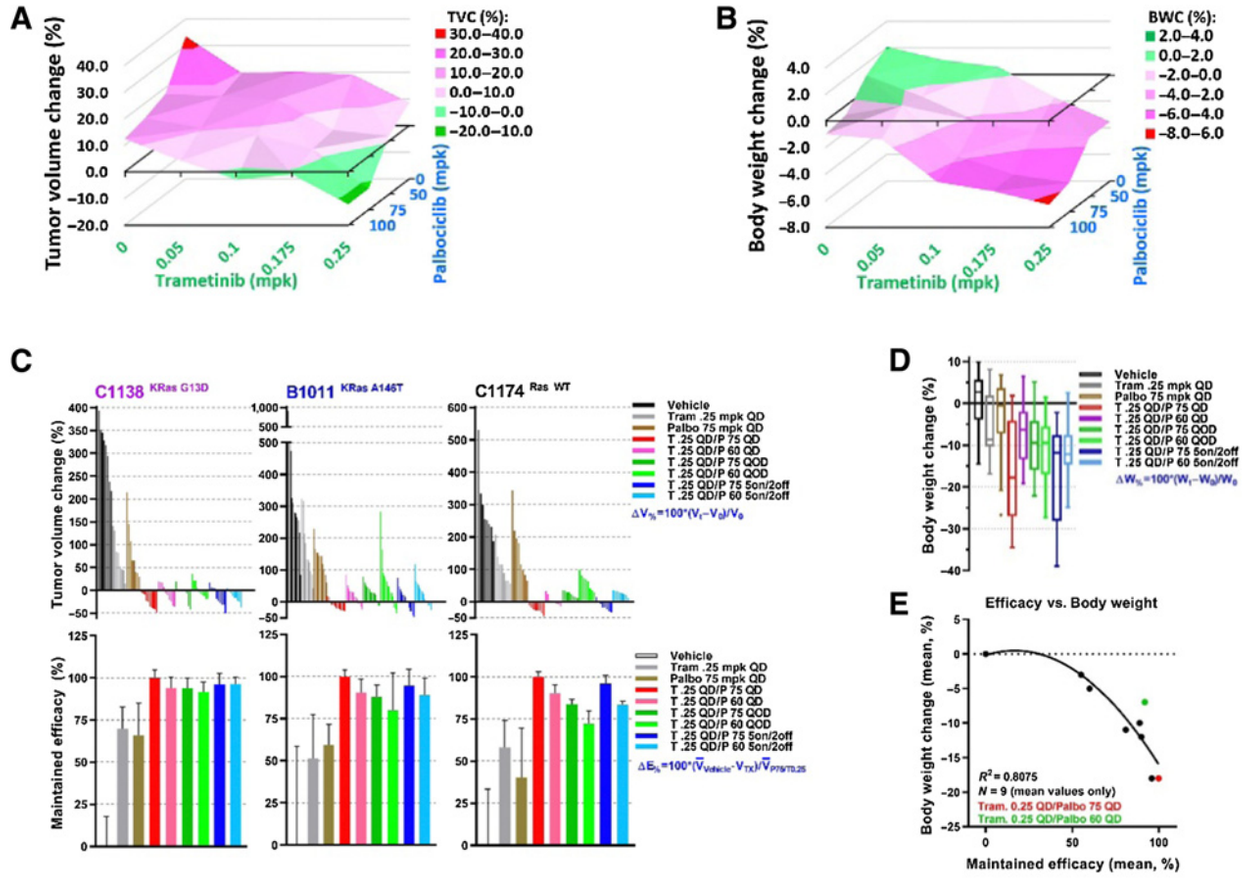

Figure 2.

Optimization of MEK and CDK4/6 combination therapy. **A,** Tumor volume changes relative to baseline [mean, $n = 3$ bilaterally implanted mice per condition (2 tumors/mouse); typical RAS^{mut} PDX C1138 was used]. **B,** Body weight changes relative to baseline (mean, $n = 3$ bilaterally implanted mice per condition). **C,** Waterfall representation of PDX models' responses (ΔV%) to alternative treatments (top set). Maintained efficacy (ΔE%, mean ±SD) of the alternative regimens relative to trametinib (0.25 mpk, daily)/palbociclib (75 mpk, daily) combination efficacy (bottom set). **D,** Effect of treatments on mice body weight [Tukey plot, after 21 days of treatment (summarized data for 3 PDX models)]. **E,** Correlation between toxicity and maintained efficacy of alternative regimens.

Mechanisms of acquired resistance to MEK and CDK4/6 inhibitors treatment

To determine the possible drug resistance mechanisms, we performed whole-exome sequencing of the resistance clones generated from continuous treatment (Supplementary Table S8). No recurrent mutations or amplifications were identified across the models (Supplementary Fig. S5A and S5B), and none of the genomic changes fit putative mechanisms of acquired resistance. Moreover, when we attempted to rechallenge these resistant clones with palbociclib/trametinib combination after several passages, all clones responded to the treatment again, indicating that the acquired resistance was indeed transient (Supplementary Fig. S5C). This observation suggests that rechallenge strategies could potentially be beneficial in the clinical setting.

To substantiate the nature of acquired resistance via the adaptive rewiring of signaling pathways, we further analyzed changes in signaling pathways after short-term (5 days) and long-term treatments (21 days) by RPPA (Supplementary Fig. S3). MAPK and RB remained inhibited at 21 days in the combination. Proteins that were significantly upregulated in palbociclib/trametinib-treated tumors (vs. single drugs) were enriched in RTK signaling, including phosphorylated HER2, VEGFR2, and IGFR ($P < 0.05$; Supplementary Fig. S5D). Concomitantly, phospho-Akt and its downstream signaling molecule phospho-p70S6K were also significantly upregulated. Tested models did not have aberrations in PTEN protein. Analysis of tumors progressed on double combination revealed the activation of Src and increased phosphorylation in its downstream targets, including SHP2 (**Fig. 5E**). Aberrant Src activation has been described in multiple cancers, including colorectal cancer where approximately 80% increased expression is noted from that of the normal epithelium (25). Src inhibitors are currently evaluated in the clinic for several cancer types as multiple effectors of Src include the Ras/PI3K/Akt and Ras/Raf/MAPK, but our prior work showed that dasatinib (Src inhibitor) at achievable doses in colorectal cancer is insufficient to inhibit Src, and may not be a viable option with currently available inhibitors (26). Targeting SHP2 directly is therefore a feasible option in KRAS^{mut} colorectal cancer. Intriguingly, elevated phospho-SHP2 level was detected in 11 of 15 PDX models treated with the combination (Supplementary Fig. S5D and S5E); SHP2 inhibition has recently been shown to prevent adaptive resistance to MAPK pathway inhibitors, likely mediated by multifactorial signaling through receptor tyrosine kinases and reductions in inhibitory phosphatases under MAPK

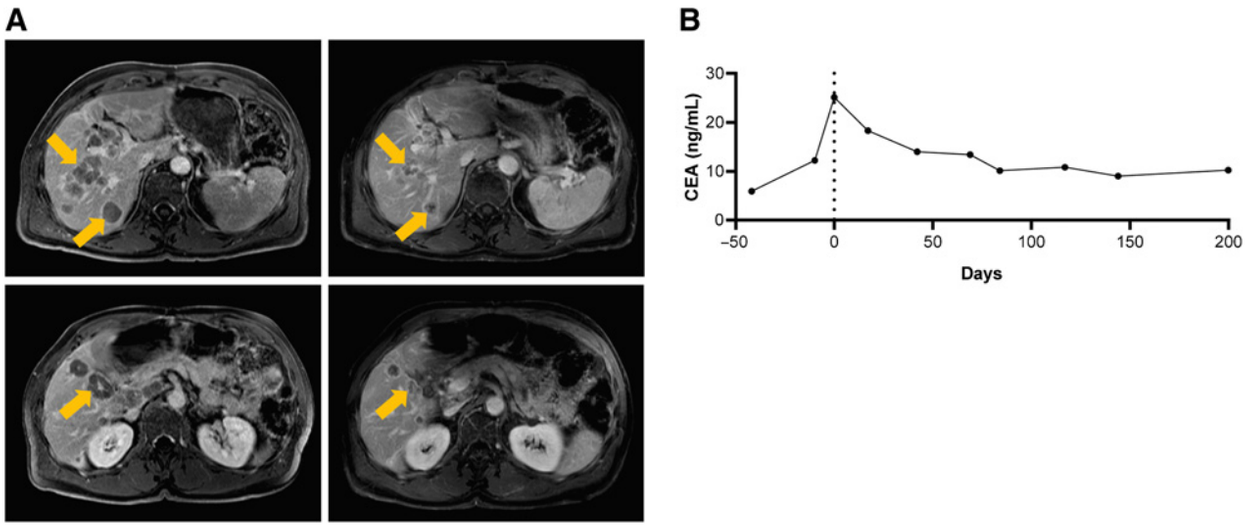

Figure 3.
Clinical response to MEK and CDK4/6 inhibition in a patient with metastatic colorectal cancer. **A,** Liver metastases as denoted by arrows at baseline (left) and after 4 months of therapy (right). **B,** Graph of carcinoembryonic antigen (CEA), with normal <3.8 ng/mL. Dotted line, initiation of therapy.

pathway control (27–29). We therefore focused on SHP2i as a potential combination therapy.

Triple combination of MEK, CDK4/6, and SHP2 inhibition in countering adaptive resistance

On the basis of these studies, we hypothesized that inhibition of SHP2 in combination with MEK/CDK4/6 inhibitors may extend palbociclib/trametinib treatment durability.

First, we evaluated the potency of combining a SHP2 inhibitor with MEK inhibitor *in vitro* using various $KRAS^{mut}$ colorectal cancer cell lines. Combinational indexes shown in **Fig. 5A** were <1, which suggested a greater than additive drug response in all of the cell lines. The combination was also effective in attenuating colony formation compared with single agents (**Fig. 5B**).

For SHP2 inhibitor combination evaluation *in vivo*, we selected two PDXs (B1008 and F3008) and treated them with the triple combination of MEK + CDK4/6 + SHP2 inhibitors. In both models, the triple combination was numerically more efficacious than the double combination, but only the F3008 model demonstrated statistical significance (**Fig. 5C**). The combination caused modest weight loss in mice that was experimentally manageable (**Fig. 5D**). Activated SHP2 levels rapidly increased in F3008 model after just 5 days of treatment (**Fig. 5E**) and also acquired resistance to MEK/CDK4/6 inhibitors combination more rapidly than B1008 (**Fig. 5F** and **G**). In contrast, B1008 model had lower basal level of activated SHP2 and showed no upregulation in 5 or 21 day treated samples but only after resistance formation (**Fig. 5E**, PD). Consistent with this, in both models, after acquiring resistance to MEK + CDK4/6 inhibitors, the addition of a SHP2 inhibitor induced rapid tumor regression (**Fig. 5F** and **G**). With the addition of SHP2 inhibitor we observe an inhibition in the feedback elevation of phosphor-AKT as expected (**Fig. 5H**).

Discussion

Targeting colorectal cancers with KRAS and NRAS mutations represent a key unmet need and important drug development priority, but is limited by tumor heterogeneity, adaptive resistance, and narrow therapeutic windows for combination therapies. Mindful of this complexity, we used a coclinical trial design with clinically relevant PDX models to evaluate therapeutic strategies focused on targeting multiple signaling nodes. Prior work had suggested the synergistic effects of using MEK and CDK4/6 inhibitor combination in $KRAS^{mut}$ colorectal cancer *in vitro* and *in vivo* (14, 30), prompting the investigation of this combination in the clinic for various cancer types (31). Previous work has identified the MAPK pathway as a mediator of tumor cell survival despite CDK4/6 inhibition, providing further rational for deeper exploration of the combination (32). Therefore, we undertook an assessment of the breadth of activity and mechanisms of response and resistance in a co-clinical trial, and evaluated the combination in patients with RAS^{mut} colorectal cancer.

In this work, we demonstrate preclinical activity of the combination of MEK and CDK4/6 inhibition in PDX models and early evidence of activity in a patient. The co-clinical trial met its primary endpoint of demonstrating tumor regressions in greater than 30% of models, with a tolerable regimen in the mice. We were able to translate this into the clinic using an alternative MEK inhibitor of binimetinib and palbociclib, with acceptable safety profile and early signal of activity. On the basis of this, an investigator-initiated randomized phase II study of binimetinib and palbociclib versus trifluridine/tipiracil (TAS-102) is being conducted. It is notable that there was activity in a limited number of RAS^{WT} models, suggesting the potential to further explore this in EGFR inhibitor refractory population.

The strengths of a co-clinical trial include the ability to estimate the activity across the spectrum of colorectal cancer biology, isolate the impact of individual components in each model, and the ability to identify potential predictive biomarkers that can be confirmed in patient samples. The combination of MEK and CDK4/6 inhibition was effective and demonstrated greater tumor regression than the single agents in most models. However, the duration of disease control was variable, with some models more rapidly adapting to the regimen. As duration of disease control is a key endpoint for clinical trials of refractory colorectal cancer, we explored potential predictive biomarkers of treatment duration, utilizing the consensus molecular subtypes and molecular profiles of the tumors (4). The PDX tumors used in our

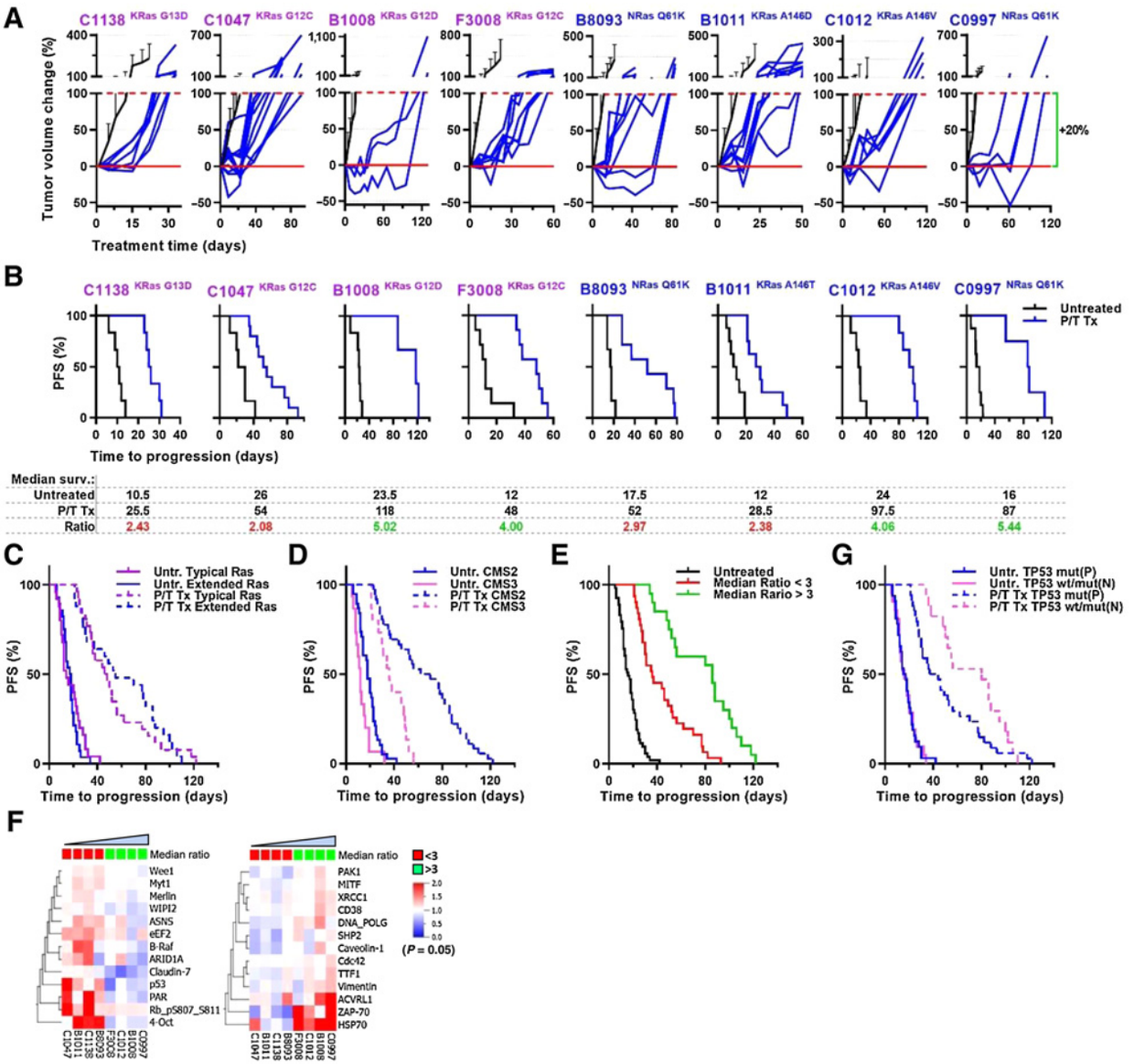

Figure 4.

Molecular characterization of trametinib/palbociclib refractory PDX models. **A,** Effect of treatments on tumor volume change. Tumors were treated with vehicle (black line; mean ± SD; $n = 6$–9 tumors), or trametinib/palbociclib combination (0.25/60 mpk, 5 days ON/2 days OFF; blue lines, individual tumors). **B,** Kaplan–Meier analysis per model. PFS was determined as a time until tumor volume doubling ($\Delta V = 100\%$, or $+20\%$ RECIST). **C–E** and **G,** Kaplan–Meier analysis (summarized data for all models): data stratified by RAS subtypes (**C**), data stratified by CMS (**D**), data stratified by median PFS ratio (vehicle vs. palbociclib/trametinib treated; **E**), data stratified by TP53 mutational status (**G**). **F,** Baseline protein levels in PDX models of proteins that significantly overexpressed (left) or underexpressed (right) in PDX models with shorter relative duration of response to the palbociclib/trametinib treatment (by median PFS ratio; mean, $n = 3$ tumor samples per model; $P < 0.05$, two-group comparison).

study were predominantly generated from treatment refractory metastatic tumors with microsatellite stability and predominantly of CMS2 and CMS3 types. While the CMS3 subtype is less common than CMS2 and CMS4, it is enriched in KRAS mutations (33). We demonstrate that CMS2 was associated with a longer duration of disease control. It should be noted that CMS4 is heavily influenced by stromal infiltrates, the mixed murine stromal and human epithelium precluded a full assessment of the CMS4 biology in this study. An additional finding was the association of TP53 mutations with shorter disease control, although these conclusions are limited by the small sample size. Although we do not validate these potential predictive findings in an alternate dataset, on the basis of this work, we have integrated assessment of CMS and TP53 in the translational plan for the randomized phase II study. Other intriguing potential predictive biomarkers include claudin-7 and OCT4. We found that claudin-7 expression to be upregulated in PDXs that showed shorter durability. This finding is consistent with previously reported studies showing that increased claudin-7 expression inversely correlates with disease-

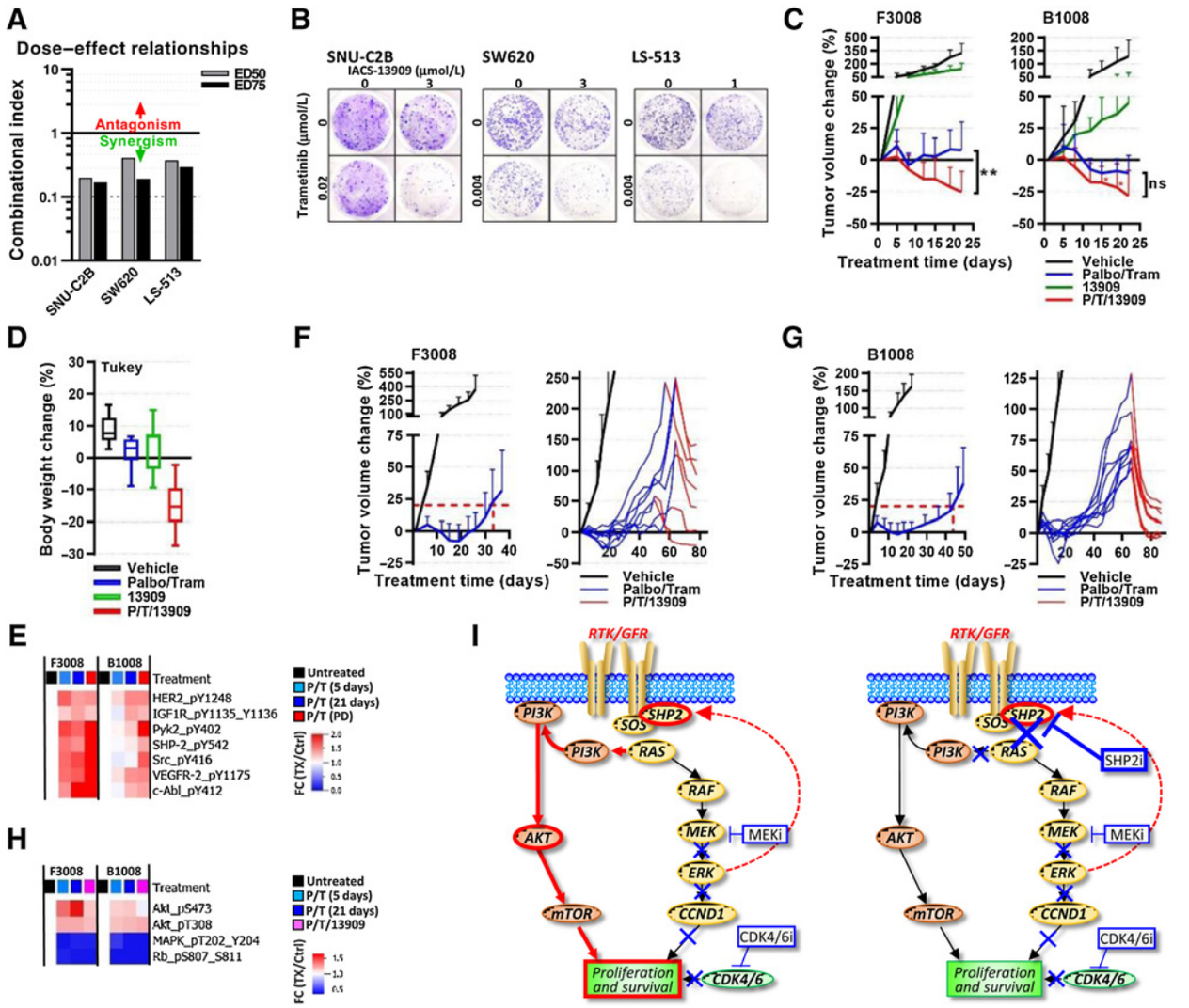

Figure 5.

Evaluation efficacy of combination with SHP2 inhibitor. **A,** Viability of KRAS^{mut} cell lines treated with trametinib, Navire 13909 (SHP2 inhibitor), or their combination for 72 hours was analyzed by XTT (mean ± SD, $n = 3$) and used for combinational effects analysis. Combinational indexes at ED_{50} and ED_{75} are indicated. **B,** Colony formation assay of KRAS^{mut} cell lines treated with DMSO, trametinib, Navire 13909, or their combination (concentrations of drugs as indicated) for 14 days. Cells were stained with crystal violet. **C,** Effect of treatments on tumor volume change (mean ± SD; $n = 4$–5 tumors per arm). Trametinib/palbociclib combination (0.25 mpk, daily/60 mpk, daily; green), Navire 13909 (SHP2 inhibitor, 40 mpk, QOD; blue), and their combination (red) were evaluated in F3008 and B1008 mCRC PDX models. ns, not significant, $P > 0.05$; **, $P \leq 0.01$. **D,** Effect of treatments on mice body weight. Tukey plot, after 21 days of treatment. Summarized data for two PDX models. **E,** Protein expression level in F3008 and B1008 PDX models after indicated time of treatment [5 days, 21 days or until ΔV = 20% (PD)] with trametinib/palbociclib combination (0.25 mpk, daily/75 mpk, daily). Protein levels (mean, $n = 3$ per treatment) were normalized to the mean of vehicle-treated control ($n = 3$; $P < 0.05$). **F** and **G,** Effect of treatments on tumor volume change. Left, trametinib/palbociclib combination (0.25 mpk, daily/75 mpk, daily; blue), vehicle (black; mean ± SD; $n = 6$–8 tumors per arm; right, vehicle (mean ± SD; $n = 6$–8 tumors per arm; black), trametinib/palbociclib combination (0.25 mpk, daily/75 mpk, daily; blue), trametinib/palbociclib/13909 combination (0.25 mpk, daily/60 mpk, daily/30 mpk, QOD; red). Each line, individual tumor. **H,** Protein expression level in F3008 and B1008 PDX models after indicated time of treatment [5 days, 21 days or until ΔV = 20% (PR)] with trametinib/palbociclib/13909 combination (0.25 mpk, daily/75 mpk, daily/30 mpk, QOD). Protein levels (mean, $n = 3$ per treatment) were normalized to the mean of vehicle-treated control ($n = 3$; $P < 0.05$). **I,** Schematic representation of RTK/RAS and PI3K signaling pathways and combinational strategies. Left, an overview of signaling pathways changes under prolong MEK/CDK4/6 inhibitors treatment. Right, rationale of using SHP2 inhibitor in tumors with acquired resistance to trametinib/palbociclib combination.

free survival and confers higher resistance to apoptosis in colorectal cancers (34). In addition, we found that overexpression of OCT4 is also a predictor of shorter durability. In various preclinical/clinical studies, high OCT4 expression of either mRNA or protein was associated with poor clinical outcome and associated with chemoresistance in the majority of cancers (reviewed in ref. 35). It should be noted that our preclinical data also suggests a role for the MEK/CDK4/6 combination in KRAS/NRAS^{WT} tumors as well, however the compelling clinical need and straightforward development path in RAS^{mut} tumors has guided the current clinical trial plans.

Recognizing the potential limitations of tolerability of the combination, we used mouse modeling to assess the toxicity and efficacy

tradeoffs of various dosing regimens and dose levels. Using mouse weight and white blood cell counts as a surrogate for toxicity, we developed a strategy to guide dose reductions in the phase IB/II study to optimize risk/benefit. While the surrogacy of murine models for assessing toxicity in patients is not robust, this provided some rationale for an evidenced-based approach to optimize the starting dose and subsequent dosing adjustments (**Fig. 2**). We were able to demonstrate a therapeutic window in patients, albeit in only 6 patients, consistent with and guided by the ongoing NSCLC study of binimetinib and palbociclib, (NCT03170206). The predominant side effects are consistent with the underlying components. It remains to be seen whether the exposures of palbociclib utilized in the mouse models will translate to the doses safely achieved in the clinic. As we demonstrate, reduction in palbociclib or binimetinib exposure is associated with loss of efficacy and we would predict less efficacy in the clinic than seen in the co-clinical trial as a result of these differences. Nevertheless, this combination has demonstrated very preliminary evidence of activity and tolerability in the patients in the safety lead-in and is worthy of further exploration.

As duration of disease control is a key determinant of benefit from targeted therapies in colorectal cancer, we also investigated the mechanisms of acquired resistance to the inhibition of MEK1/2, CDK4/6, or their combination. In contrast to the observation in melanoma patients of acquired resistance through outgrowth of a $PIK3CA^{mut}$ clone (36), molecular analysis of these emergent resistant tumors/clones to MEK/CDK4/6 inhibitors long-term therapy suggested that they do not harbor any new oncogenic mutations, nor do share potentially oncogenic CNVs (Supplementary Table S9). Instead, our results uncovered the adaptive modulation of RAS signaling networks leading to reactivation of the pathway, with identification of SHP2 as a potential candidate that can be targeted to significantly delay or prevent the resistance mechanisms (**Fig. 5I**). On the basis of this finding, we then added a SHP2 inhibitor at the time of progression on MEK/CDK4/6 inhibitors, resulting in tumor regressions (**Fig. 5F** and **G**). This finding is consistent with a study in $NRAS^{mut}$ melanomas resistance to MEK1/2 and CDK4/6 inhibition upregulated activity of the RTK/RAS/RAF and RTK/PI3K/AKT signaling cascade (37). Several studies and ongoing clinical trials are exploring the use of SHP2 inhibitors in cancer therapy, and it remains to be seen if a therapeutic window would be possible to enable a triplet combination as suggested by our data (38–40).

In conclusion, this study suggests the activity of CDK4/6 and MEK dual inhibition in RAS^{mut} colorectal cancer tumors in a coclinical trial with a diversity of PDX models and in patients with metastatic colorectal cancer, identified potential biomarkers of response, and demonstrated the role of SHP2-mediated signaling in acquired resistance to the regimen. This study highlights the potential opportunities from formal co-clinical trials of combination previously established prior to, or in parallel with, early clinical studies. We identified potential predictive biomarkers of benefit, and identify targetable mechanisms of adaptive resistance at progression. Together, these results will inform and accelerate rationale combination therapy for patients with RAS^{mut} metastatic colorectal cancer.

Authors' Disclosures

B. Johnson reports personal fees from Taiho Oncology, Insmed Oncology, Gritstone bio, and Incyte, grants from BMS, other support from Syntrix, and grants from Gateway for Cancer Research outside the submitted work. V.K. Morris reports other support from BioNTech, Pfizer, Bristol Myers Squibb, EMD Serono, and Novartis outside the submitted work. P. Jones reports a patent for US20170342078 issued and licensed to Navire Pharma. M.S. Lee reports personal fees from Delcath, Imvax, and G1 Therapeutics, grants and personal fees from Pfizer, grants from Amgen, nonfinancial support from Bristol-Myers Squibb, grants from EMD Serono, Exelixis, Genentech/Roche, Rafael Pharmaceuticals, Arcus Biosciences, Shanghai EpimAb Biotherapeutics, and Repare outside the submitted work. S. Kopetz reports other support from MolecularMatch, Lutris, Iylon, Genentech, EMD Serono, Merck, Holy Stone, Novartis, Lilly, Boehringer Ingelheim, Boston Biomedical, AstraZeneca/MedImmune, Bayer Health, Pierre Fabre, Redx Pharma, Ipsen, Daiichi Sankyo, Natera, HalioDx, Lutris, Jacobio, Pfizer, Repare Therapeutics, Inivata, GlaxoSmithKline, Jazz Pharmaceuticals, Iylon, Xilis, Abbvie, Amal Therapeutics, Gilead Sciences, Mirati Therapeutics, Flame Biosciences, Servier, Carina Biotechnology, Bicara Therapeutics, Endeavor BioMedicines, Numab Pharma, Johnson & Johnson/Janssen, Sanofi, Biocartis, Guardant Health, Array BioPharma, Genentech/Roche, EMD Serono, MedImmune, Novartis, Amgen, Lilly, and Daiichi Sankyo during the conduct of the study. No disclosures were reported by the other authors.

Authors' Contributions

A.V. Sorokin: Conceptualization, data curation, formal analysis, supervision, validation, investigation, visualization, methodology, writing–original draft, project administration, writing–review and editing. **P. Kanikarla Marie:** Conceptualization, formal analysis, validation, investigation, visualization, methodology, writing–original draft, project administration, writing–review and editing. **L. Bitner:** Validation, investigation, methodology. **M. Syed:** Validation, investigation, methodology. **M. Woods:** Validation, investigation, methodology. **G. Manyam:** Software, formal analysis, investigation, visualization, methodology, writing–original draft. **L.N. Kwong:** Software, formal analysis, visualization, methodology, writing–original draft. **B. Johnson:** Conceptualization, resources, data curation, formal analysis, funding acquisition, investigation, methodology, writing–original draft, project administration, writing–review and editing. **V.K. Morris:** Conceptualization, resources, data curation, formal analysis, supervision, funding acquisition, investigation, methodology, writing–original draft, project administration, writing–review and editing. **P. Jones:** Conceptualization, resources. **D.G. Menter:** Conceptualization, resources, data curation, formal analysis, supervision, funding acquisition, investigation, methodology, writing–original draft, project administration, writing–review and editing. **M.S. Lee:** Conceptualization, resources, data curation, formal analysis, supervision, funding acquisition, investigation, methodology, writing–original draft, project administration, writing–review and editing. **S. Kopetz:** Conceptualization, resources, data curation, formal analysis, supervision, funding acquisition, investigation, visualization, methodology, writing–original draft, project administration, writing–review and editing.

Acknowledgments

This study was supported by NIH through both the Cancer Center Support Grant P30CA16672, SPORE Grant P50CA221707, U54CA224065-02S1, 5R01CA184843-05, and supported by the generous philanthropic contributions to UT MD Anderson Cancer Center Moon Shots Program as well as The Del and Dennis McCarthy Distinguished Professorship. In addition, UT MD Anderson Cancer Center's RPPA Core, which is supported by NCI Grant CA16672 and Yiling Lu's NIH Grant R50CA221675. Clinical trial is supported by Pfizer.

The costs of publication of this article were defrayed in part by the payment of page charges. This article must therefore be hereby marked *advertisement* in accordance with 18 U.S.C. Section 1734 solely to indicate this fact.

Note

Supplementary data for this article are available at Cancer Research Online (http://cancerres.aacrjournals.org/).

Received January 18, 2022; revised May 20, 2022; accepted July 26, 2022; published first August 1, 2022.

References

1. Siegel RL, Miller KD, Goding Sauer A, Fedewa SA, Butterly LF, Anderson JC, et al. Colorectal cancer statistics, 2020. CA Cancer J Clin 2020;70:145–64.
2. Hobbs GA, Wittinghofer A, Der CJ. Selective targeting of the KRAS G12C mutant: kicking KRAS when it's down. Cancer Cell 2016;29:251–3.

3. Guinney J, Dienstmann R, Wang X, de Reynies A, Schlicker A, Soneson C, et al. The consensus molecular subtypes of colorectal cancer. Nat Med 2015;21: 1350–6.
4. Sawayama H, Miyamoto Y, Ogawa K, Yoshida N, Baba H. Investigation of colorectal cancer in accordance with consensus molecular subtype classification. Ann Gastroenterol Surg 2020;4:528–39.
5. Lievre A, Bachet JB, Le Corre D, Boige V, Landi B, Emile JF, et al. KRAS mutation status is predictive of response to cetuximab therapy in colorectal cancer. Cancer Res 2006;66:3992–5.
6. Loupakis F, Ruzzo A, Cremolini C, Vincenzi B, Salvatore L, Santini D, et al. KRAS codon 61, 146 and BRAF mutations predict resistance to cetuximab plus irinotecan in KRAS codon 12 and 13 wild-type metastatic colorectal cancer. Br J Cancer 2009;101:715–21.
7. Fearon ER. Molecular genetics of colorectal cancer. Annu Rev Pathol 2011;6: 479–507.
8. Pupo E, Avanzato D, Middonti E, Bussolino F, Lanzetti L. KRAS-driven metabolic rewiring reveals novel actionable targets in cancer. Front Oncol 2019;9:848.
9. Ryan MB, Corcoran RB. Therapeutic strategies to target RAS-mutant cancers. Nat Rev Clin Oncol 2018;15:709–20.
10. Lanman BA, Allen JR, Allen JG, Amegadzie AK, Ashton KS, Booker SK, et al. Discovery of a covalent inhibitor of KRAS(G12C) (AMG 510) for the treatment of solid tumors. J Med Chem 2020;63:52–65.
11. Pantsar T. The current understanding of KRAS protein structure and dynamics. Comput Struct Biotechnol J 2020;18:189–98.
12. Rubin SM, Sage J, Skotheim JM. Integrating old and new paradigms of G1/S control. Mol Cell 2020;80:183–92.
13. Kwong LN, Costello JC, Liu H, Jiang S, Helms TL, Langsdorf AE, et al. Oncogenic NRAS signaling differentially regulates survival and proliferation in melanoma. Nat Med 2012;18:1503–10.
14. Lee MS, Helms TL, Feng N, Gay J, Chang QE, Tian F, et al. Efficacy of the combination of MEK and CDK4/6 inhibitors in vitro and in vivo in KRAS mutant colorectal cancer models. Oncotarget 2016;7:39595–608.
15. Ziemke EK, Dosch JS, Maust JD, Shettigar A, Sen A, Welling TH, et al. Sensitivity of KRAS-mutant colorectal cancers to combination therapy that cotargets MEK and CDK4/6. Clin Cancer Res 2016;22:405–14.
16. Inoue A, Deem AK, Kopetz S, Heffernan TP, Draetta GF, Carugo A. Current and future horizons of patient-derived xenograft models in colorectal cancer translational research. Cancers 2019;11:1321.
17. Shi J, Li Y, Jia R, Fan X. The fidelity of cancer cells in PDX models: characteristics, mechanism and clinical significance. Int J Cancer 2020;146:2078–88.
18. Prasetyanti PR, van Hooff SR, van Herwaarden T, de Vries N, Kalloe K, Rodermond H, et al. Capturing colorectal cancer inter-tumor heterogeneity in patient-derived xenograft (PDX) models. Int J Cancer 2019;144:366–71.
19. Schueler J, Tschuch C, Klingner K, Bug D, Peille AL, de Koning L, et al. Induction of acquired resistance towards EGFR inhibitor gefitinib in a patient-derived xenograft model of non-small cell lung cancer and subsequent molecular characterization. Cells 2019;8:740.
20. Katsiampoura A, Raghav K, Jiang ZQ, Menter DG, Varkaris A, Morelli MP, et al. Modeling of patient-derived xenografts in colorectal cancer. Mol Cancer Ther 2017;16:1435–42.
21. Julien S, Merino-Trigo A, Lacroix L, Pocard M, Goéré D, Mariani P, et al. Characterization of a large panel of patient-derived tumor xenografts representing the clinical heterogeneity of human colorectal cancer. Clin Cancer Res 2012; 18:5314–28.
22. Hong DS, Morris VK, El Osta B, Sorokin AV, Janku F, Fu S, et al. Phase IB study of vemurafenib in combination with irinotecan and cetuximab in patients with metastatic colorectal cancer with BRAFV600E mutation. Cancer Discov 2016;6: 1352–65.
23. Poulin EJ, Bera AK, Lu J, Lin YJ, Strasser SD, Paulo JA, et al. Tissue-specific oncogenic activity of KRAS(A146T). Cancer Discov 2019;9:738–55.
24. Bera AK, Lu J, Wales TE, Gondi S, Gurbani D, Nelson A, et al. Structural basis of the atypical activation mechanism of KRAS(V14I). J Biol Chem 2019;294:13964–72.
25. Hurwitz H, Fehrenbacher L, Novotny W, Cartwright T, Hainsworth J, Heim W, et al. Bevacizumab plus irinotecan, fluorouracil, and leucovorin for metastatic colorectal cancer. N Engl J Med 2004;350:2335–42.
26. Parseghian CM, Parikh NU, Wu JY, Jiang ZQ, Henderson L, Tian F, et al. Dual inhibition of EGFR and c-Src by cetuximab and dasatinib combined with FOLFOX chemotherapy in patients with metastatic colorectal cancer. Clin Cancer Res 2017;23:4146–54.
27. Ruess DA, Heynen GJ, Ciecielski KJ, Ai J, Berninger A, Kabacaoglu D, et al. Mutant KRAS-driven cancers depend on PTPN11/SHP2 phosphatase. Nat Med 2018;24:954–60.
28. Fedele C, Ran H, Diskin B, Wei W, Jen J, Geer MJ, et al. SHP2 inhibition prevents adaptive resistance to MEK inhibitors in multiple cancer models. Cancer Discov 2018;8:1237–49.
29. Sun Y, Meyers BA, Czako B, Leonard P, Mseeh F, Harris AL, et al. Allosteric SHP2 inhibitor, IACS-13909, overcomes EGFR-dependent and EGFR-independent resistance mechanisms toward osimertinib. Cancer Res 2020;80: 4840–53.
30. Posch C, Sanlorenzo M, Ma J, Kim ST, Zekhtser M, Ortiz-Urda S. MEK/CDK4,6 co-targeting is effective in a subset of NRAS, BRAF and 'wild type' melanomas. Oncotarget 2018;9:34990–5.
31. Scheiblecker L, Kollmann K, Sexl V. CDK4/6 and MAPK-crosstalk as opportunity for cancer treatment. Pharmaceuticals 2020;13:418.
32. de Leeuw R, McNair C, Schiewer MJ, Neupane NP, Brand LJ, Augello MA, et al. MAPK reliance via acquired CDK4/6 inhibitor resistance in cancer. Clin Cancer Res 2018;24:4201–14.
33. Smeby J, Sveen A, Merok MA, Danielsen SA, Eilertsen IA, Guren MG, et al. CMS-dependent prognostic impact of KRAS and BRAFV600E mutations in primary colorectal cancer. Ann Oncol 2018;29:1227–34.
34. Kuhn S, Koch M, Nübel T, Ladwein M, Antolovic D, Klingbeil P, et al. A complex of EpCAM, claudin-7, CD44 variant isoforms, and tetraspanins promotes colorectal cancer progression. Mol Cancer Res 2007;5:553–67.
35. Mohiuddin IS, Wei SJ, Kang MH. Role of OCT4 in cancer stem-like cells and chemotherapy resistance. Biochim Biophys Acta Mol Basis Dis 2020;1866: 165432.
36. Romano G, Chen P-L, Song P, McQuade JL, Liang RJ, Liu M, et al. A preexisting rare *PIK3CA*^{E545K} subpopulation confers clinical resistance to MEK plus CDK4/6 inhibition in *NRAS* melanoma and is dependent on S6K1 signaling. Cancer Discov 2018;8:556–67.
37. Hayes TK, Luo F, Cohen O, Goodale AB, Lee Y, Pantel S, et al. A functional landscape of resistance to MEK1/2 and CDK4/6 inhibition in NRAS-mutant melanoma. Cancer Res 2019;79:2352–66.
38. Butterworth S, Overduin M, Barr AJ. Targeting protein tyrosine phosphatase SHP2 for therapeutic intervention. Future Med Chem 2014;6:1423–37.
39. Mullard A. Phosphatases start shedding their stigma of undruggability. Nat Rev Drug Discov 2018;17:847–9.
40. Scott LM, Lawrence HR, Sebti SM, Lawrence NJ, Wu J. Targeting protein tyrosine phosphatases for anticancer drug discovery. Curr Pharm Des 2010;16:1843–62.